Optimum and standard beam widths for numerical modeling of interface scattering problems

Ralph A. Stephen[a]
Woods Hole Oceanographic Institution, Woods Hole, Massachusetts 02543

Gaussian beams provide a useful insonifying field for surface or interface scattering problems such as encountered in electromagnetics, acoustics and seismology. Gaussian beams have these advantages: (i) They give a finite size for the scattering region on the interface. (ii) The incident energy is restricted to a small range of grazing angles. (iii) They do not have side lobes. (iv) They have a convenient mathematical expression. The major disadvantages are: (i) Insonification of an interface is nonuniform. The scattered field will depend on the location of the scatterers within the beam. (ii) The beams spread, so that propagation becomes an integral component of the scattering problem. A standard beam parameterization is proposed which keeps propagation effects uniform among various models so that the effects of scattering only can be compared. In continuous wave problems, for a given angle of incidence and incident amplitude threshold, there will be an optimum Gaussian beam which keeps the insonified area as small as possible. For numerical solutions of pulse beams, these standard parameters provide an estimate of the smallest truncated domain necessary for a physically meaningful result. © *2000 Acoustical Society of America.* [S0001-4966(00)05202-4]

PACS numbers: 43.20.Bi, 43.20.Fn, 43.30.Gv, 43.30.Hw [ANN]

INSONIFYING FIELDS FOR SCATTERING PROBLEMS

Many representations of scattering functions are based on the notion of an incident plane wave (Bass and Fuks, 1979; Beckman and Spizzichino, 1963; Felsen and Marcuvitz, 1973; Ishimaru, 1978; Ogilvy, 1991). To avoid edge effects at non-normal angles of incidence and to localize the scattering area on the interface, however, some form of tapering at the edges of the plane wave is often employed in theoretical approaches (Pott and Harris, 1984; Thorsos, 1988; Zeroug and Felsen, 1994, for example), numerical approaches (Hastings *et al.*, 1995; Jensen and Schmidt, 1987; Stephen and Swift, 1994; for example) and in laboratory experiments (Breazeale *et al.*, 1977; Chimenti *et al.*, 1994; Muir *et al.*, 1979, for example). In numerical scattering formulations, particularly, it is important to minimize the insonified area to keep computer memory and computation times as small as possible. In this paper we use the Gaussian beam description given by Červený *et al.* (1982) to predict the minimum width of a two-dimensional continuous wave (cw) beam for a given grazing angle and incident amplitude threshold. Since in numerical solutions to wave scattering and propagation problems it is advantageous to keep the computational domain as small as possible, the ''minimum'' width beams are considered ''optimum.'' An extension of this parameterization to pulse beams leads to a definition of standard beams for validity testing and benchmark models.

The concept of an infinite plane wave as the incident field originates from Fresnel reflection coefficient theory (Jackson, 1975, Sec. 7.3) in electromagnetics, and similar treatments for plane wave reflection coefficients in acoustics (Pierce, 1989, Sec. 3.6) and seismology (Aki and Richards, 1980, Sec. 5.2). In these cases, semi-infinite plane waves are incident on infinite planar surfaces separating semi-infinite half-spaces. When coupled with the plane or cylindrical wave decomposition of a point source (Aki and Richards, 1980, Chap. 6; Sommerfeld, 1909; Von Weyl, 1919), the reflection coefficients can be used to solve the problem of a point source over a planar interface separating two semi-infinite media. In seismology these are referred to as Lamb's problems (Lamb, 1904). All of these problems are well posed notions completely consistent with the wave equations. The propagation and scattering (reflection and transmission) are both correct simultaneously. The solutions are exact and they lead to a number of convenient and powerful concepts in wave theory such as wave number vector decompositions.

However, problems arise when truncating the time and space domains. The integral transforms can no longer be evaluated to infinity and the convenient concepts only apply approximately over certain bandwidths or in given spatial domains. Scattering problems from surface roughness and volume heterogeneities introduce ''length scales'' to the problem which are not present in the problems of Fresnel, Lamb, Weyl, and Sommerfeld. In stratified media or in the geometrical optics (high frequency) limit, the introduction of a length scale is not a problem if one is careful in defining the bandwidth and the smoothness (wave number content) of the medium. In scattering theory for infinite surfaces with small stochastic roughness or for infinite surfaces with periodic discrete scatterers, it is still valid to consider incident and scattered semi-infinite plane waves. If the domain is truncated, however, either explicitly by tapering the incident field (Thorsos, 1988, for example) or implicitly by adding a single discrete scattering element on the interface, semi-infinite plane waves are no longer well posed. It is at this point that the trade-off between angle resolution and spatial resolution is introduced if one wants to do both the propaga-

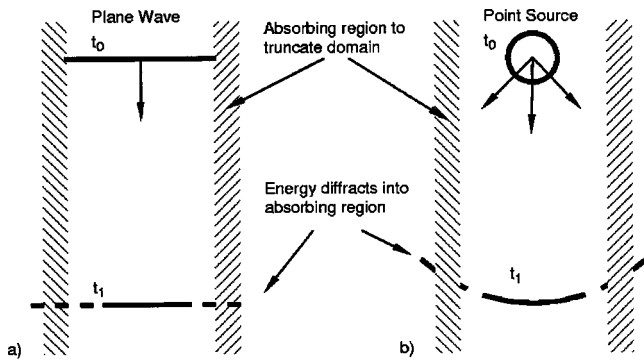---

[a]Electronic mail: rstephen@whoi.edu

FIG. 1. In some numerical solutions to wave equations, such as time-domain finite-differences, it is necessary to make the computational domain in space as small as possible. This is accomplished by adding absorbing regions (hashed) around the spatial domain of interest. The examples in (a) and (b) show a truncated plane wave and a point source, respectively, propagating in a homogeneous medium. Because of diffraction of energy into the absorbing region, neither of these examples correctly portrays propagation in infinite, homogeneous media. Similar but less obvious effects occur in many applications where the medium is more complex. As an alternative to plane waves and point sources, Gaussian beams provide a convenient and useful incident field in these cases of dramatically truncated domains.

tion and scattering problems simultaneously. Large domains permit small angle spread and small domains require larger angle spread. Gaussian beams provide a mechanism to address this trade-off quantitatively.

This study has been motivated by the computational necessity, in time-domain numerical solutions to wave equations, to keep the spatial and temporal domains as small as possible. Spatial domains of only a few hundred wavelengths on a side in two-dimensional problems or only a few tens of wavelengths on a side for three-dimensional problems challenge even the fastest and largest computers. It is tempting to use spatial domains that are so small or have such a narrow aspect ratio that even results for homogeneous media will not be valid.

As an example, consider propagation in a homogeneous, two-dimensional medium (Fig. 1). Figure 1(a) is an example similar to acoustic well logging problems. The incident field is a vertically propagating plane wave, but in an effort to minimize the computational domain absorbing boundaries are placed close together and parallel to the propagation direction. In this case energy diffracts from the edges of the plane wave into the absorbing regions on either side. After propagating a short distance, the planar wave front inside the domain no longer agrees with the intended solution of an infinite plane wave. This problem is closely related to the radiated field from a vibrating piston (Pierce, 1989, Chap. 5). Figure 1(b) is an example similar to many problems in controlled source or earthquake modeling. It shows a point source in homogeneous media where the domain has been truncated by absorbing boundaries parallel to the propagation direction of interest. This is often done in an effort to minimize the computational domain. In this problem, energy also diffracts into the absorbing boundaries, and the solutions for even homogeneous media will be incorrect. Although these examples are trivial, similar but less obvious effects occur in many applications where the medium is more complex.

I. GAUSSIAN BEAMS

Gaussian beams are a useful way to restrict the angular (or horizontal wave number) content of the incident field while keeping the interaction localized on the surface (Červený et al., 1982; Chimenti et al., 1994; Felsen, 1976). However, by truncating a plane wave the additional complexity of beam spreading (Huygen's principle) must be considered. This introduces propagation issues into scattering problems.

In this paper we are interested in actual Gaussian beams in homogeneous media which can be used as insonifying fields for scattering problems (Bertoni and Tamir, 1973; Choi and Harris, 1989; Felsen, 1976; Jensen and Schmidt, 1987; Zeroug and Felsen, 1994, for example). There is extensive literature on the Gaussian beam summation method for computing wave fields from point and line sources in inhomogeneous media (Červený et al., 1982; George et al., 1987; Klimeš, 1989; Nowack and Aki, 1984; Weber, 1988; White et al., 1987, for example). The Gaussian beam summation method is not being addressed here. Rather we consider Gaussian beams as a physical reality.

Assume that the medium is homogeneous and that we are in a two-dimensional Cartesian coordinate system. For a beam waist centered at (x_p, z_p) with a half-width at the waist of L_M, and an angle of incidence α, the pressure at (x,z) is given by (Červený et al., 1982),

$$\Phi(x,z) = \sqrt{\frac{\sqrt{2\pi}L_M}{s+\epsilon}} \exp\{2\pi i[s+n^2/(2(s+\epsilon))]\},$$

where

$$\epsilon = -i\pi L_M^2,$$

$$s = (x-x_p)\sin(\alpha) + (z-z_p)\cos(\alpha),$$

$$n = (x-x_p)\cos(\alpha) - (z-z_p)\sin(\alpha). \quad (1)$$

This is an asymptotic solution to the time harmonic, two-dimensional parabolic wave equation, obtained using a parabolic approximation to the wave equation about the beam axis. The beam coordinates are (s, n), where s is the propagation distance from the beam waist and n is the direction normal to the beam axis (Fig. 2). All distances are in terms of wavelengths. The normalized power, the area under $|\Phi|^2$ as a function of wavelength across the beam, is unity. If Φ is pressure (in Pascals), ρ is density (in kg/m³) and f is frequency (in Hertz), then the power in the beam (in Watts) is

$$P = \frac{1}{\rho f} \int |\Phi|^2 dn = \frac{1}{\rho f}. \quad (2)$$

An equation similar to Eq. (1), with differences in the phase and amplitude normalization, can also be derived using the complex source point method (Zeroug and Felsen, 1994).

In ray coordinates, Eq. (1) can be rewritten as

$$\Phi(s,n) = \sqrt{\frac{\sqrt{2\pi}L_M}{s-i\pi L_M^2}} \exp\left\{2\pi i[s+n^2 K(s)] - \frac{n^2}{L^2(s)}\right\},$$
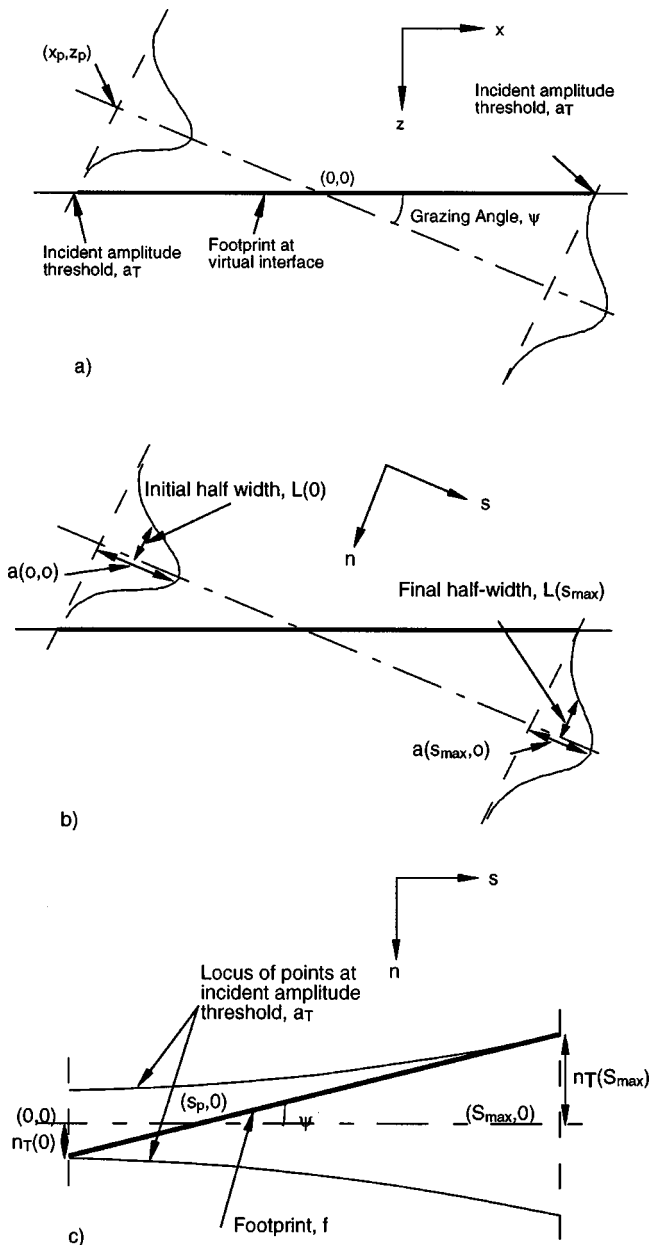
where

FIG. 2. (a) The optimum Gaussian beam for surface scattering problems is defined on the notion that the beam will spread as it propagates across a flat virtual interface at the mean level of the surface. Optimum beam parameters are constrained by the grazing angle and the incident amplitude threshold. The incident amplitude threshold is the maximum acceptable incident amplitude at the edges of the scattering region and is chosen based on an acceptable level of artifacts from edge effects. The minimum half-width occurs at the beam waist. The origin is defined as the intersection of the beam axis and the virtual interface. The center of the beam waist is located at (x_p, z_p). The footprint size is the distance along the virtual interface between the lower and upper incident amplitude threshold points. (b) To compute parameters for the optimum beam it is convenient to work in beam coordinates (s,n). Two parameters that define the shape of the beam are the incident amplitude threshold, a_T, and the propagation distance, S_{max}. From these one can compute the half-width at the beam waist, $L(0)$, the size of the footprint on the virtual interface, f, and the "nominal" angle of incidence, ψ. By the inverse coordinate transform in Eq. (1) one can also locate the beam waist in (x,z) coordinates, (x_p, z_p). (c) The locus of points which have an amplitude a_T is shown in beam coordinates.

$$K(s) = \frac{s}{2[s^2 + (\pi L_M^2)^2]},$$

$$L(s) = \sqrt{L_M^2 + \left(\frac{1}{\pi L_M}\right)^2 s^2}. \quad (3)$$

$K(s)$ controls the divergence of the beam energy or curvature of the surfaces of constant phase. The profile of the beam is Gaussian with an "effective half-width," $L(s)$. This is the half-width to the point where the amplitude decreases to e^{-1} of the value which occurs at the beam axis. The function $L(s)$ defines the beam envelope as a half-width and is hyperbolic. If the beam envelope is defined by an absolute amplitude, however, there is a small additional factor to account for the change in amplitude along the beam axis. The amplitude of the beam is

$$a(s,n) = \sqrt{\frac{\sqrt{2\pi}L_M}{\sqrt{s^2 + (\pi L_m^2)^2}}} \exp\left\{-\frac{n^2}{L^2(s)}\right\}. \quad (4)$$

The power on lines normal to the beam is constant and the amplitude on the beam axis, $a(s,0)$, is related to the half-width, $L(s)$, by

$$a^2(s,0)L(s) = \sqrt{\frac{2}{\pi}}. \quad (5)$$

For a given path length, S_{max}, in homogeneous media there is an initial beam half-width, L_M^{opt}, which will yield the narrowest beam, as defined by half-width

$$L_M^{opt} = \sqrt{S_{max}/\pi}. \quad (6a)$$

The corresponding half-width at S_{max} is

$$L(S_{max}) = \sqrt{2S_{max}/\pi}. \quad (6b)$$

Gaussian beams are a convenient incident field for interface scattering problems because they have such a simple analytic expression for the beam divergence and they have a predictable minimum width for a given propagation distance. For initial beam half-widths less than L_M^{opt}, the beam spreads more, so that the half-width at S_{max} is greater than $\sqrt{2S_{max}/\pi}$. For initial beam half-widths greater than L_M^{opt}, the beam spreads less but the resultant half-width at S_{max} is still greater than $\sqrt{2S_{max}/\pi}$.

Bessel beams have many of the same advantages as Gaussian beams and, in addition, they are diffraction-free and do not spread (Durnin and Miceli, 1988). The major disadvantage of Bessel beams for interface scattering problems is that they have multiple lobes and zeros within the beam. Insonification across the beam footprint is dramatically nonuniform.

Felsen and coauthors (Chimenti *et al.*, 1994; Felsen, 1984; Zeroug and Felsen, 1992) use the complex source point (CSP) method to generate beams which are close approximations to plane waves with a Gaussian profile when the Fresnel length [πL_M^2 in Eq. (1)] is greater than a wavelength. The beam is constructed by interference of evanescent (inhomogeneous) plane waves. Their approach has been applied to the study of reflection of Gaussian beams from fluid loaded elastic structures (Chimenti *et al.*, 1994) and the coupling of beams to leaky modes (Zeroug and Felsen, 1994). Good agreement between the CSP method and laboratory observations was obtained (Chimenti *et al.*, 1994).

A number of investigators have used bounded beams to study reflection and refraction at planar fluid-solid interfaces (Bertoni and Tamir, 1973; Breazeale *et al.*, 1977; Pott and

Harris, 1984, for example). Deterministic scattering of bounded beams from rough seafloors has been discussed by Stephen and Swift (1994), from volume heterogeneities below a fluid-solid boundary by Swift and Stephen (1994), and from a rough sea surface by Thorsos (1996), Stephen (1996) and Hastings *et al.* (1997). In this paper we propose a standard beam configuration for all types of interface and surface scattering problems including flat interfaces between homogeneous media, interfaces with volume heterogeneity in the lower medium, interfaces with fine scale roughness and interfaces with discrete scatterers.

II. THE "OPTIMUM" GAUSSIAN BEAM

When applying Gaussian beams to interface scattering problems it is desirable to minimize the footprint on the interface while keeping the half-width of the beam, the amplitude of the incident field, and the angle of incidence as constant as possible across the footprint. The "optimum" Gaussian beam is defined by considering propagation in a homogeneous medium with the beam incident on a virtual interface normal to the z axis in a Cartesian coordinate system [Fig. 2(a)]. The virtual interface is transparent to the optimum beam. The virtual interface, however, specifies the location of the mean surface for actual scattering problems and is the reference for defining the beam parameters.

We choose the origin in (x,z) coordinates to be at the intersection of the axis of the beam and the virtual interface. The beam axis intersects the virtual interface with the nominal grazing angle, ψ. Since the beam diverges as it propagates across the virtual interface [because of the curvature factor $K(s)$ in Eq. (3)], the actual grazing angle [defined in this context as the inverse cosine of the slope of the phase curve in cycles per wavelength (Stephen, 1996)] varies with range along the interface.

For a given angle of incidence and a given incident amplitude threshold, the optimum Gaussian beam will minimize the insonified area, or footprint, on the virtual surface. The incident amplitude threshold, a_T, is the largest incident amplitude that is acceptable at the end of the tapers on the left and right edges of the scattering region [Fig. 2(a)]. It can be expressed in decibels down from a reference amplitude,

$$\hat{A}_T = 20 \log_{10}(\hat{a}_T) = 20 \log_{10}\left(\frac{a_T}{a(0,0)}\right). \tag{7}$$

For a reference amplitude we choose the peak amplitude at the beam waist, $a(0,0)$, which in homogeneous media is the largest amplitude in the problem. (In this paper we use $\log_{10}$ to indicate logarithms to the base 10 and log to indicate natural logarithms.) As the beam propagates along its axis from the waist, its half-width, $L(s)$, increases and its on-axis amplitude, $a(s,0)$, decreases according to Eqs. (3) and (5). The normalized amplitude, $\hat{a}$, can be expressed in terms of the waist half-width only,

$$\hat{a}(s,n) = \sqrt{\frac{\pi L_M^2}{\sqrt{s^2 + (\pi L_M^2)^2}}} \exp\left\{\frac{-n^2}{L^2(s)}\right\},$$

$$L^2(s) = L_M^2 + \left(\frac{1}{\pi L_M}\right)^2 s^2. \tag{8}$$

The beam half-width from the axis to the normalized amplitude $\hat{a}$ is

$$n(s) = \pm \left(L_M^2 + \left(\frac{s}{\pi L_M}\right)^2 \right)^{1/2} \left[-\log(\hat{a}) \right. $$
$$\left. -\log\left(\sqrt{\frac{\sqrt{s^2 + (\pi L_M^2)^2}}{\pi L_M^2}} \right) \right]^{1/2}. \tag{9}$$

The first expression on the right side represents the hyperbolic spreading of the beam half-width corresponding to an amplitude of $1/e$. The first term in the square brackets modifies the $1/e$ half-width to the half-width at the normalized amplitude. The second term in square brackets allows for the decay in amplitude along the beam axis. For a fixed distance, s, the term in square brackets varies much more slowly with respect to the waist half-width, than the preceding hyperbolic spreading term. The waist half-width which gives the narrowest beam in terms of half-width [Eq. (6)] also gives the narrowest beam in terms of constant amplitude. The beam half-width to the normalized amplitude can then be expressed as a function of the propagation distance, $S_{\max}$,

$$n(s) = \pm \left(\frac{S_{\max}^2 + s^2}{\pi S_{\max}}\right)^{1/2} \left[-\log\left(\hat{a} \sqrt{\frac{\sqrt{S_{\max}^2 + s^2}}{S_{\max}}} \right) \right]^{1/2}. \tag{10}$$

To compute parameters for the optimum beam it is convenient to work in beam coordinates, (s,n) [Fig. 2(b)]. The beam shape is defined by the locus of points at the amplitude threshold, $\hat{a}_T$. The beam half-width, from the axis to the amplitude threshold, is $n_T(s)$. The angle that the beam axis makes with the virtual interface is the grazing angle, ψ. The initial and final beam half-widths, $n_T(0)$ and $n_T(S_{\max})$, are

$$n_T(0) = \pm \sqrt{\frac{S_{\max}}{\pi}(-\log \hat{a}_T)},$$

$$n_T(S_{\max}) = \pm \sqrt{\frac{2S_{\max}}{\pi}(-\log \hat{a}_T - \log \sqrt[4]{2})}. \tag{11}$$

Now tan ψ is the sum of these initial and final beam half-widths divided by the propagation distance, $S_{\max}$ [Fig. 2(c)]. So for a given grazing angle and a given incident amplitude threshold, the propagation distance for the optimum Gaussian beam can be obtained,

$$S_{\max} = \frac{\left[\sqrt{-\log \hat{a}_T} + \sqrt{2(-\log \hat{a}_T - \log \sqrt[4]{2})}\right]^2}{\pi \tan^2 \psi}. \tag{12}$$

Once $S_{\max}$ is determined, the waist half-width is obtained by (6) and the beam shape is defined by (3). The footprint on the virtual interface, f, is

$$f = \frac{S_{\max}}{\cos \psi}. \tag{13}$$

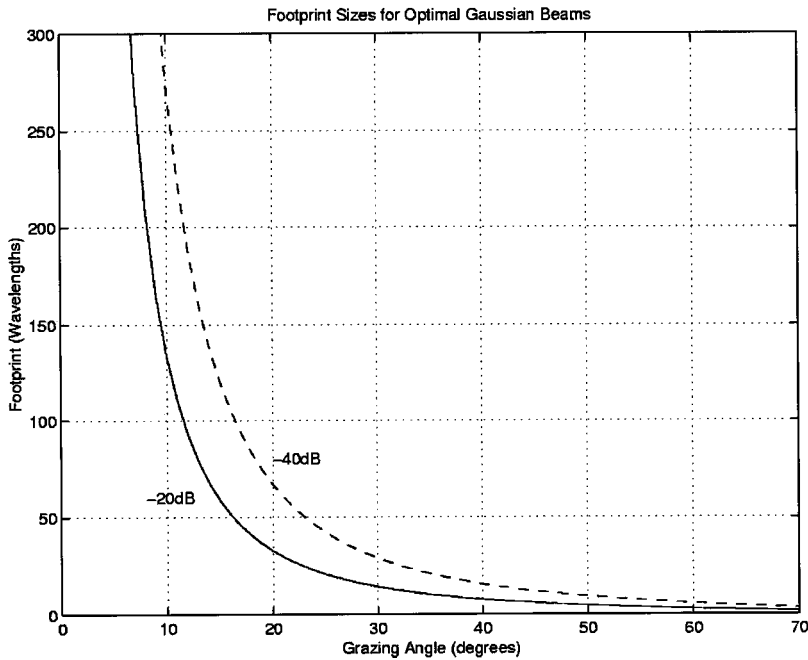Footprint Sizes for Optimal Gaussian Beams

FIG. 3. Footprint sizes are shown as a function of grazing angle for amplitude threshold values of -20 and -40 dB. Using minimum footprints is particularly important at low grazing angles where the footprint size exceeds 100 wavelengths. At higher grazing angles, where the optimum footprint size goes to zero, other issues may constrain the footprint size. For example, it may be necessary to have a sufficiently large number of scattering elements on the interface to adequately represent the statistical distribution of scatterers. Since angle spread increases with decreasing beam waist widths, defining the beam in terms of grazing angle and acceptable angle spread may be more useful.

The center of the beam waist in (x,z) coordinates, (x_p, z_p) is

$$x_p = -n_T(0) \frac{\cos \psi}{\tan \psi}, \quad z_p = -n_T(0) \cos \psi, \quad (14)$$

Footprint sizes as functions of grazing angle for the optimum Gaussian beams are shown in Fig. 3 for incident amplitude thresholds of -20 and -40 dB. For thresholds less than -20 dB, footprints greater than 130 wavelengths are necessary for grazing angles less than about 10°. For thresholds greater than -40 dB, at grazing angles near 50° the footprints drop below about 10 wavelengths. At grazing angles greater than 50° there will be criteria other than beam spreading which control the footprint size. For example, one needs a footprint sufficiently large that there will be enough scattering elements to adequately represent a particular phenomenon. Since angle spread increases with decreasing beam waist widths, defining beams in terms of grazing angle and acceptable angle spread may be more useful.

III. EXAMPLES AND DISCUSSION

As an example of an optimum Gaussian beam, consider a 400 Hz beam insonifying a surface at 10° grazing angle in water (velocity of 1500 m/s, density of 1000 kg/m³) (Fig. 4). This is similar to the incident field used in Test Case 1 of Thorsos (1996) which was generated by a vertical array. Gaussian beams for Test Case 1 are also discussed in Stephen (1996). Figure 5 shows the projection of the incident optimum Gaussian beam on the surface for an incident amplitude threshold of -40 dB. The footprint size is 1023 m

(273 wavelengths) compared to the 750 m (200 wavelengths) footprint used in Test Case 1. Figure 6 shows the corresponding grazing angle across the surface. Even though the nominal grazing angle was 10°, the actual grazing angle varies from about 7 to 10.5°. The angle spread for the optimum Gaussian beam of 3.5° is narrower by about 1° than the angle spread for the beam used in Test Case 1. The waist half-width of the optimum beam is 34.68 m and is considerably wider than the half-width of the vertical taper used in Test Case 1, 27.55 m. The depth of the midpoint of the waist is also deeper, 73.30 compared to 66.12 m. [The ''optimum Gaussian beam'' discussed in Stephen (1996) was based on slant range, rather than the amplitude threshold criteria defined in Eq. (12). This gave a more meaningful comparison with the other beams discussed in that paper but was not as rigorous in terms of incident amplitude constraints.]

In some formulations of the scattering problem (Hastings *et al.*, 1995; Thorsos, 1988, for example), the incident field is ''layed-down'' on the scattering surface, rather than propagating the incident field up to the scattering surface. The scattered fields are compared with theoretical results for incident plane waves. Gaussian tapers, however, are used on the mean scattering surface to truncate the domain, and the incident field in the medium adjacent to the scattering surface is undefined and could be quite complicated. Comparison with results from other methods, where it is impractical to ''lay-down'' the incident field, would be difficult. In these formulations, the optimum Gaussian beams defined here would provide useful incident fields with simple and well-
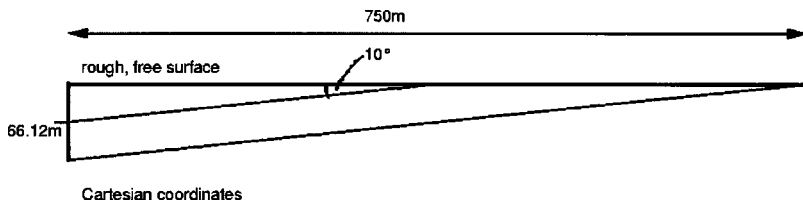

FIG. 4. As an example of an optimum beam calculation, consider a 400 Hz beam insonifying a free surface at 10° grazing angle in water (velocity of 1500 m/s, density of 1000 kg/m³).
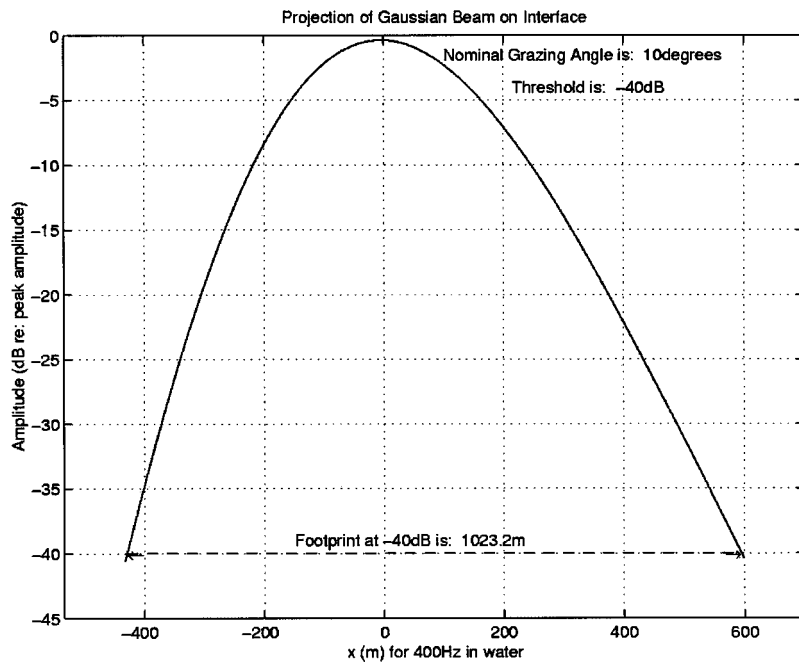
FIG. 5. The optimum beam projection on the interface for the example shown in Fig. 4 has a footprint of over 1000 m for an incident threshold value of −40 dB. If beam spreading were ignored and geometrical optics was used to project the beam, the footprint size would be only 750 m. The projection of the Gaussian beam on the horizontal surface is asymmetrical because of beam spreading.

defined propagation characteristics. In one example, Hastings *et al.* (1995) for a rough sea surface with a grazing angle of 10° used a footprint of 180 wavelengths and a halfwidth for the Gaussian taper of 40 wavelengths. The optimum Gaussian beam with an incident amplitude threshold of −36 dB has a footprint of 245 wavelengths and the profile on the footprint has a half-width of about 54 wavelengths. It is beyond the scope of this paper to investigate the numerical implications of using optimum Gaussian beams in these methods, but it would be worth considering them. The optimum beam profile could be used in these calculations with very little additional computational effort. In addition to having the propagation of the incident field well defined, the angle spread over the footprint would also be well defined. In this case it is less than 3.5°.

In a third example, Stephen and Swift (1994) use a Gaussian pulse-beam as the insonifying field for seafloor scattering problems in a Numerical Scattering Chamber using time-domain finite-differences. Their footprint calculations assume a uniform "channel width," rather than a minimum incident amplitude threshold. The optimum Gaussian beam, based on the peak frequency in pressure, for a grazing angle of 15° and an incident amplitude threshold of −20 dB, would have a waist half-width of 4.25 wavelengths located at (−23.27, −6.24). The footprint would be only 58.9 wavelengths compared to the 72 wavelengths used in the earlier study. The depth of the computational domain would not change appreciably, but there would be a reduction in the length by 20% and computational time would be reduced by 35% for the same problem. The divergence, caused by the
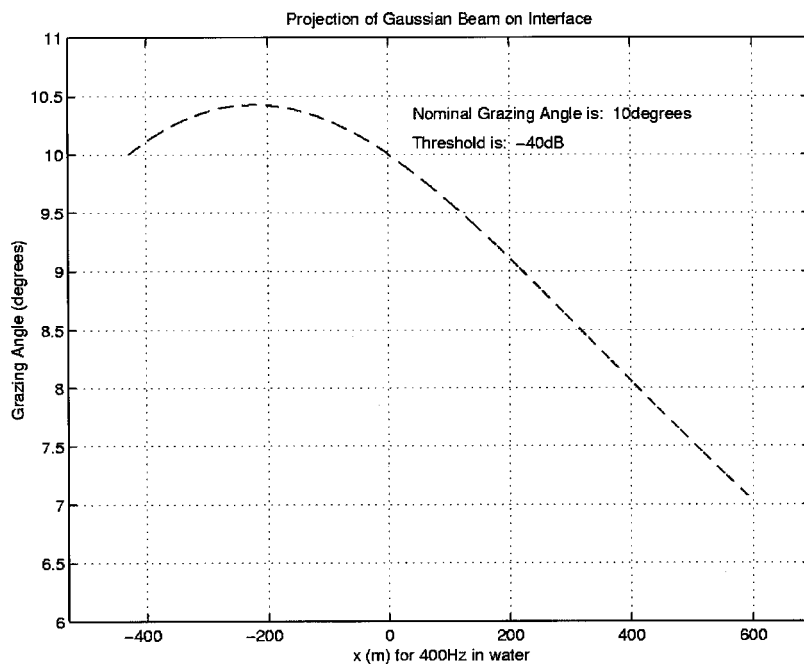

FIG. 6. Grazing angles for the optimum Gaussian beam in Fig. 4, with a nominal grazing angle of 10°, actually vary from about 7.0 to 10.5°. Narrower angle ranges (less diffraction) can be obtained by using wider footprints.

TABLE I. Frequency effects on beam parameters.

At $s=0$:	$L(0)$-meters	$\hat{a}(0,n_T(0))$
Peak frequency (10 Hz)	638.1	0.1000
Upper half-power frequency (13.6 Hz)	638.1	0.0707
Lower half-power frequency (6.8 Hz)	638.1	0.0707
At $s=S_{max}$:	$L(S_{max})$-meters	$\hat{a}(S_{max},n_T(S_{max}))$
Peak frequency (10 Hz)	902.4	0.1000
Upper half-power frequency (13.6 Hz)	792.8	0.0402
Lower half-power frequency (6.8 Hz)	1132	0.1373

curvature of the phase fronts, of the optimum Gaussian beam would be about 5°.

In a Gaussian pulse-beam the various frequency components of the beam will spread at different rates. For the same initial half-width and propagation distance (in meters, not wavelengths), lower frequency beams will spread more. Table I shows half-widths and normalized amplitude thresholds at the peak frequency and upper and lower half-power frequencies for the time wavelet used in Stephen and Swift (1994). The table assumes a peak frequency of 10 Hz and a propagation velocity of 1500 m/s. At the lower half-power frequency the beam has spread 25% more, and the threshold amplitude at $[S_{max},n_T(S_{max})]$ is 37% greater than at the peak frequency. If these discrepancies are judged to be significant, a more conservative value of the incident amplitude threshold should be used in the beam design.

By considering Gaussian beams as the incident field, we gain some insight into the problem of backscatter in the limit as grazing angle goes to zero. It is challenging to imagine a plane wave incident on an interface at 0° grazing angle. It is quite natural, however, to consider a Gaussian beam, such as in Fig. 2(c), propagating at 0° just above an interface with a particular incident amplitude threshold. The optimum beam notion, discussed above, would not apply, but the incident field into the interface would consist solely of diffracted energy from beam spreading. The insonified length between incident amplitude thresholds would still be bounded because of decay in amplitude along the beam axis. Scattering elements, either roughness on the interface or sub-bottom heterogeneity, would scatter a finite amount of energy back into the upper medium in all directions.

Although in this paper we considered Gaussian beams in two-dimensional media, a similar approach can be taken to obtain optimum beams for interface scattering problems in three dimensions using the formulas for three-dimensional Gaussian beams (Červený, 1985, Sec. 9; Pott and Harris, 1984; Wang and Waltham, 1995; Zeroug and Felsen, 1994, for example).

IV. CONCLUSIONS

In applying cw Gaussian beams to seafloor scattering problems there are optimum beam parameters which minimize the size of the scattering region on the interface. For a given footprint size, these optimum Gaussian beams have the most uniform half-width and the least angle spread across the footprint. The optimum beam parameters are constrained by the angle of incidence and the incident amplitude threshold. In finite bandwidth, pulse-beam problems, standard beams

can be defined by applying the optimum beam parameters at the peak or center frequencies. By using optimum Gaussian beams investigators can minimize and standardize the propagation effects in beam scattering problems.

Aki, K., and Richards, P. G. (**1980**). *Quantitative Seismology: Theory and Methods* (Freeman, San Francisco), Vol. 1.

Bass, F. G., and Fuks, I. M. (**1979**). *Wave Scattering from Statistically Rough Surfaces* (Pergamon, Oxford).

Beckman, P., and Spizzichino, A. (**1963**). *The Scattering of Electromagnetic Waves from Rough Surfaces* (Pergamon, Oxford).

Bertoni, H. L., and Tamir, T. (**1973**). ''Unified theory of Rayleigh-Angle phenomena for acoustic beams at liquid-solid interfaces,'' Appl. Phys. **2**, 157–172.

Breazeale, M. A., Alder, L., and Scott, G. W. (**1977**). ''Interaction of ultrasonic waves incident at the Rayleigh angle onto a liquid-solid interface,'' J. Appl. Phys. **48**, 530–537.

Červený, V. (**1985**). ''The application of ray tracing to the numerical modeling of seismic wavefields in complex structures,'' in *Seismic Shear Waves, Part A: Theory, Handbook of Geophysical Exploration*, edited by G. Dohr (Geophysical, London), Vol. 15A, pp. 1–124.

Červený, V., Popov, M. M., and Pšenčík, I. (**1982**). ''Computation of wave fields in inhomogeneous media—Gaussian beam approach,'' Geophys. J. R. Astron. Soc. **70**, 109–128.

Chimenti, D. E., Zhang, J.-G., Zeroug, S., and Felsen, L. B. (**1994**). ''Interaction of acoustic beams with fluid-loaded elastic structures,'' J. Acoust. Soc. Am. **95**, 45–59.

Choi, H.-C., and Harris, J. G. (**1989**). ''Scattering of an ultrasonic beam from a curved interface,'' in *Wave Motion II*, edited by N. Holland (Elsevier Science, New York), pp. 383–406.

Durnin, J., and Miceli, Jr., J. (**1988**). ''Comparison of Bessel and Gaussian beams,'' Opt. Lett. **13**, 79–80.

Felsen, L. B. (**1976**). ''Complex-point-source solutions of the field equations and their relation to the propagation and scattering of Gaussian beams,'' in *Symposia Matematica*, edited by Istituto Nazionale di Alta Matematica (Italy) (Academic, New York), Vol. 18, pp. 39–56.

Felsen, L. B. (**1984**). ''Geometrical theory of diffraction, evanescent waves, complex rays and Gaussian beams,'' Geophys. J. R. Astron. Soc. **79**, 77–88.

Felsen, L. B., and Marcuvitz, N. (**1973**). *Radiation and Scattering of Waves* (Prentice-Hall, Englewood Cliffs).

George, T., Virieux, J., and Madariaga, R. (**1987**). ''Seismic wave synthesis by Gaussian beam summation: A comparison with finite differences,'' Geophysics **52**, 1065–1073.

Hastings, F. D., Schneider, J. B., and Broschat, S. L. (**1995**). ''A Monte Carlo FDTD technique for rough surface scattering,'' IEEE Trans. Antennas Propag. **43**, 1183–1189.

Hastings, F. D., Schneider, J. B., and Broschat, S. L. (**1997**). ''A finite-difference time-domain solution to scattering from a rough pressure-release surface,'' J. Acoust. Soc. Am. **102**, 3394–3400.

Ishimaru, A. (**1978**). *Wave Propagation and Scattering in Random Media* (Academic, New York).

Jackson, J. D. (**1975**). *Classical Electrodynamics* (Wiley, New York).

Jensen, F. B., and Schmidt, H. (**1987**). ''Subcritical penetration of narrow Gaussian beams into sediments,'' J. Acoust. Soc. Am. **82**, 574–579.

Klimeš, L. (**1989**). ''Optimization of the shape of Gaussian beams of a fixed length,'' Stud. Geophys. Geod. **33**, 146–163.

Lamb, H. (**1904**). ''On the propagation of tremors over the surface of an elastic solid,'' Philos. Trans. R. Soc. London, Ser. A **203**, 1–42.

Muir, T. G., Horton, Sr., C. W., and Thompson, L. A. (**1979**). ''The penetration of highly directional acoustic beams into sediments,'' J. Sound Vib. **64**, 539–551.

Nowack, R., and Aki, K. (**1984**). ''The 2-D Gaussian beam synthetic method testing and application,'' J. Geophys. Res. **89**, 7797–7819.

Ogilvy, J. A. (**1991**). *Theory of Wave Scattering from Random Rough Surfaces* (Adam Hilger, Bristol).

Pierce, A. D. (**1989**). *Acoustics: An Introduction to its Physical Principles and Applications* (Acoustical Society of America, Woodbury).

Pott, J., and Harris, J. G. (**1984**). ''Scattering of an acoustic Gaussian beam from a fluid-solid interface,'' J. Acoust. Soc. Am. **76**, 1829–1838.

Sommerfeld, A. (**1909**). ''Uber die ausbreitung der wellen in der drahtlosen telegraphie,'' Ann. Phys. (Leipzig) **28**, 665–736.

Stephen, R. A. (**1996**). ''Modeling sea surface scattering by the time-domain finite difference method,'' J. Acoust. Soc. Am. **100**, 2070–2078.

Stephen, R. A., and Swift, S. A. (**1994**). ''Modeling seafloor geoacoustic interaction with a numerical scattering chamber,'' J. Acoust. Soc. Am. **96**, 973–990.

Swift, S. A., and Stephen, R. A. (**1994**). ''The scattering of a low-angle pulse beam by seafloor volume heterogeneities,'' J. Acoust. Soc. Am. **96**, 991–1001.

Thorsos, E. I. (**1988**). ''The validity of the Kirchhoff approximation for rough surface scattering using a Gaussian roughness spectrum,'' J. Acoust. Soc. Am. **83**, 78–92.

Thorsos, E. I. (**1996**). ''Test Case 1: Sea surface forward scattering,'' in *Benchmark Solutions in Reverberation and Scattering: Proceedings of the Reverberation and Scattering Workshop, May 2–5, 1994*, edited by D. B. King, S. A. Chin-Bing, J. A. Davis, and R. B. Evans, Naval Research Laboratory Book Contribution NRL/BE/7181-96-001 (U.S. Government Printing Office), pp. 3.2–3.20.

Von Weyl, H. (**1919**). ''Ausbretung elektromagnetischer wellen uber einen ebenen leiter,'' Ann. Phys. (Leipzig) **60**, 481–500.

Wang, T. K., and Waltham, D. A. (**1995**). ''Seismic modelling over 3-D homogeneous layered structures-summation of Gaussian beams,'' Geophys. J. Int. **122**, 161–174.

Weber, M. (**1988**). ''Computation of body-wave seismograms in absorbing 2-D media using the Gaussian beam method: Comparison with exact methods,'' Geophys. J. **92**, 9–24.

White, B. S., Norris, A., Bayliss, A., and Burridge, R. (**1987**). ''Some remarks on the Gaussian beam summation method,'' Geophys. J. R. Astron. Soc. **89**, 579–636.

Zeroug, S., and Felsen, L. B. (**1992**). ''Multiple reflected beam synthesis of fields excited by a high-frequency oblique beam input in an elastic plate,'' J. Acoust. Soc. Am. **91**, 2016–2024.

Zeroug, S., and Felsen, L. B. (**1994**). ''Nonspecular reflection of two- and three-dimensional acoustic beams from fluid-immersed plane-layered elastic structures,'' J. Acoust. Soc. Am. **95**, 3075–3089.